

Photoacoustic Drug Delivery: The Effect of Laser Parameters on Spatial Distribution of Delivered Drug

HanQun Shangguan^{1,2}, Lee W. Casperson¹, Alan Shearin^{2,5},
Kenton Gregory^{2,4}, and Scott A. Prahl^{2,3,4}

¹Portland State University, Department of Electrical Engineering, Portland, OR 97207

²Oregon Medical Laser Center, Portland, OR 97225

³Oregon Graduate Institute, Portland, OR 97291

⁴Oregon Health Sciences University, Portland, OR 97201

⁵Palomar Medical Technologies, Inc., Beverly, MA 01915

ABSTRACT

Photoacoustic drug delivery is a technique for delivering drugs to localized areas by timing laser-induced pressure transients to coincide with a bolus of drug. This study explores the effects of target material, laser energy, absorption coefficient, fiber size, repetition rate, and number of pulses on the spatial distribution of delivered drug. A microsecond flash-lamp pumped dye laser delivered 30–100 mJ pulses through optical fibers with diameters of 300–1000 μm . Vapor bubbles were created 1–5 mm above clear gelatin targets submerged in mineral oil containing a hydrophobic dye (D&C Red#17). The absorption coefficient of the oil-dye solution was varied from 50–300 cm^{-1} . Spatially unconfined geometry was investigated. We have found that while the dye can be driven a few millimeters into the gels in both the axial and radial directions, the penetration was less than 500 μm when the gel surface remained macroscopically undamaged. Increasing the distance between the fiber tip and target, or decreasing the pulse energy reduced the extent of the delivery.

1. INTRODUCTION

Photoacoustic drug delivery (PADD) describes a process in which a drug is driven into tissue by using laser-induced acoustic pressure arising from cavitation bubble expansion and collapse. Previous studies have established cavitation bubbles may be formed in a liquid or on a solid target depending on where the laser energy is absorbed. These cavitation bubbles play an important role in pulsed laser ablation of tissue. van Leeuwen *et al.* demonstrated that the cavitation bubble made it possible to ablate tissue in a non-contact mode through a layer of blood or saline effectively and the forceful expansion of a cavitation bubble induced mechanical damage in adjacent tissue in the form of dissections.¹ Jacques *et al.* studied mass removal caused by surface evaporation and explosive vaporization of water.² A study by de la Torre and Gregory demonstrated that laser energy absorption by blood produced rapidly expanding cavitation bubbles and high-pressure acoustic transients of between 10 and 1200 atmospheres.³ In clinical trials of laser thrombolysis, Gregory suggested that the removal of thrombus might be attributed to the acoustic phenomena from vaporization and ejection of materials.⁴ However, whether the laser-induced acoustic pressure can be used to drive drugs into tissue for localized drug delivery remains to be investigated.

Correspondence: prahl@ece.ogi.edu; (503) 216–2197; <http://omlc.ogi.edu>

We recently have visualized the dynamics of PADD through flash photography.⁵ The pulsed laser energy, delivered via an optical fiber, was absorbed by the light absorbing liquid. A cavitation bubble was immediately ($\sim 1 \mu\text{s}$) formed at the fiber tip. This bubble grew to a maximal size and then collapsed several hundreds of microseconds after the laser pulse. Dye in the ambient liquid was driven into the tissue by mechanical wave pressure and acoustic transients related to the bubble expansion and collapse.

This study was initially motivated by the possibility of using laser-induced acoustic transients to drive clot-dissolving enzymes into clots or vessel walls for enhancement of laser thrombolysis. Specifically, the aim of this study has been to identify the mechanisms of PADD through investigating the effects of target material, laser energy, absorption coefficient, fiber size, repetition rate, and number of pulses on the spatial distribution of delivered drug. The preliminary results show that the delivery can be achieved by selection of suitable laser parameters, and PADD may become a promising method for localized drug delivery.

2. MATERIALS AND METHODS

2.1. Laser Delivery

A $1 \mu\text{s}$ pulsed dye laser (Palomar Medical Technologies) operating at a wavelength of 504 nm was used in this study. The laser energies varied from 30–100 mJ. The repetition rate ranged from 1–10 Hz. Pulse-to-pulse energy variation was less than 5%. Optical fibers of 300, 600, and 1000 μm core diameter were used to deliver the laser pulses into the light absorbing solution.

2.2. Preparation of Thrombus Models

The thrombus was modeled using 3.5% gelatin (60–300 bloom). The strength of the gelatin was proportional to the bloom number. The gelatin-water mixture was heated to 60° with stirring until it became clear. Liquid gelatin samples were poured into 1 cm cuvettes and cured to form 1–1.5 cm thick tissue models.

2.3. Preparation of Light Absorbing Solutions

We used solutions of a hydrophobic dye (D&C Red #17 Warner-Jenkinson Co., Inc.) in mineral oil (Paddock Laboratories, Inc.) as a model for the drug. The hydrophobic dye was used to detect delivered drug in clear gelatin because the gels were water-based and staining of the surface was undesirable. The dye was added to the mineral oil to achieve the desired absorption coefficient. The absorption coefficients of the solutions had a nearly linear relationship with the concentration of the dye in the oil: 0.0367 g of dye in 30 ml oil gave an absorption coefficient of 300 cm^{-1} at 504 nm. The absorption coefficients in our experiments varied from 50–300 cm^{-1} . The dye-oil mixture was heated to 100° with stirring until the appearance became uniform, and then cooled down to room temperature. The solution of 300 cm^{-1} was easy to saturate at room temperature. Usually, after 4 hours the dye began to precipitate, and the absorption coefficient was dropped to 250 cm^{-1} .

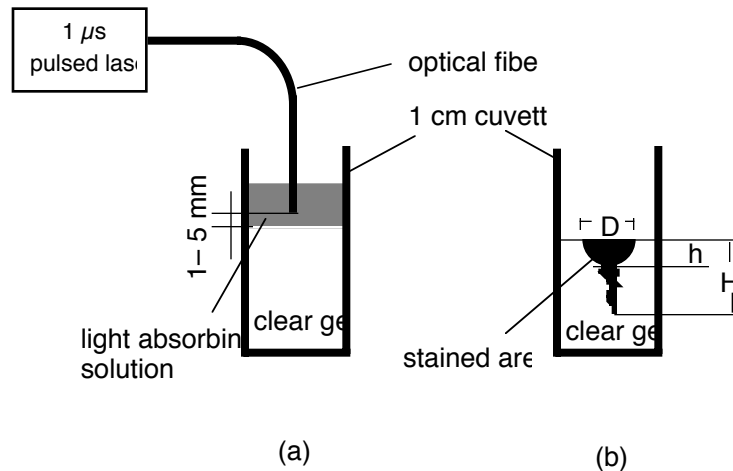


Figure 1. (a) Schematic of experimental setup. (b) Cross-section of clear gelatin after the bubble formation.

2.4. Procedures of Photoacoustic Drug Delivery

The experimental setup is outlined in Figure 1(a). The procedures of PADD are as follows:

The light absorbing solution was drawn up into a 1 cm cuvette ~ 1.5 cm on top of the clear gelatin. The cuvette was fixed with a heavy clamp to prevent displacement caused by the violent vibration associated with some laser-induced acoustic transients. Ten laser pulses were delivered through a solid glass fiber into the solution for each ablation except for the study on the effect of pulse numbers on the delivery (in this case, 10–100 pulses were delivered). The fiber tip was located 1–5 mm above the surface of the gel samples. The cavitation bubbles were formed at the fiber tip. The laser energy output was measured with a joulemeter (J50LP, Molectron Detector, Inc.) before and after each ablation. Following PADD, the samples were sectioned and measured with a stereo optical microscope (SZ6045, Olympus). The stained areas in the clear gels indicated the presence of photoacoustically delivered dye. Figure 1(b) shows how the spatial distributions of delivered drug in the gelatin were measured. The stained areas consisted of two parts: an inverted hemisphere with a diameter D and height h inserted on the surface of the gel, some colored cracks below the hemisphere.

3. RESULTS

In this study, we measured the spatial distribution of dye in clear gel samples with spatially unconfined geometry. We have found that while the dye can be driven a few millimeters into the gels in both axial (i.e., H and h) or radial (i.e., D) directions, the penetration was less than $500 \mu\text{m}$ when the gel surface remained macroscopically undamaged. The following Figures 2–8 present the results for the effects of target material, laser energy, absorption coefficient, fiber size, repetition rate, and number of pulses on the spatial distribution of delivered drug.

3.1. Spatial Distribution of Drug in Axial Direction

The penetration of drug in axial direction increases with increasing the laser energy, absorption coefficient, and pulse number, shown in Figures 3, 4, and 7. The penetration is reduced for greater strength, larger fibers, and increased distance between the fiber tip and the gel surface increase (Figures 2, 5, and 8). The repetition rate doesn't affect the spatial distribution of delivered dye, cf., Figure 6. During the ablation, we found that the dye was easily driven into the low strength gel samples. For example, the dye was driven into the weaker gel (60 bloom) after one or two pulses, while at least five pulses were needed to push the dye into the stronger gel samples (300 bloom). With increasing laser energy and absorption coefficient, a popping sound became louder due to the cavitation bubble collapse.

3.2. Spatial Distribution of Drug in Radial Direction

The penetration of drug in the radial direction is relatively independent of the laser energy, absorption coefficient, and repetition rate, but it is reduced as the strength of the gels increases. Figure 7 shows that the penetration increases significantly when the number of pulses increases. The variation in the penetration is also large when the fiber size changes. We observed that during the ablation with a $300\ \mu\text{m}$ fiber, the solution was explosively ejected and the solution in front of the fiber tip became dark, i.e., it was burnt. The ablation using a $600\ \mu\text{m}$ fiber was more violent than that using a $1000\ \mu\text{m}$ fiber, but no explosive ejection was observed.

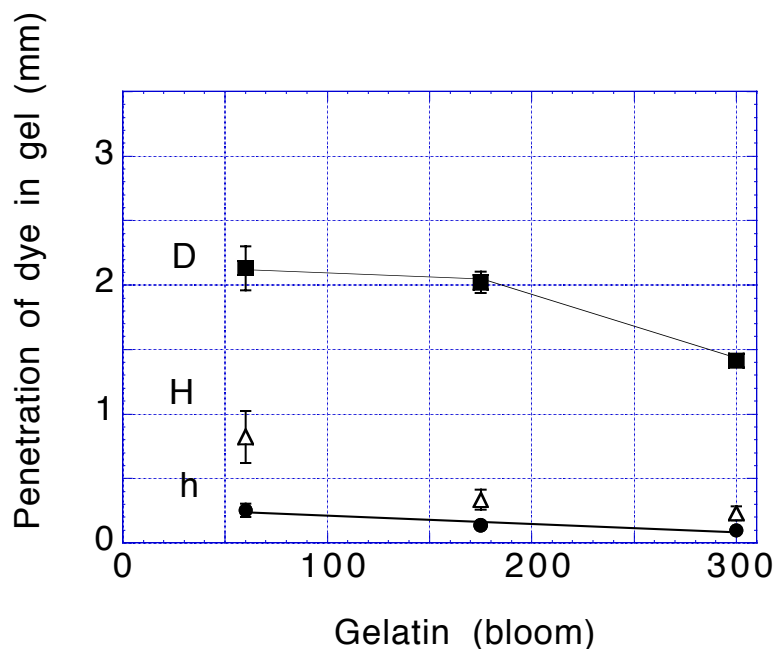


Figure 2. Effect of target materials: Penetration of dye in clear gel plotted against the gel mechanical strength. The squares (D), triangles (H), and circles (h) present the dye distributions in their own specific directions, cf., Figure 1(b). Absorption coefficient was $300\ \text{cm}^{-1}$. Ten pulses of 60 mJ laser energy at 3 Hz were delivered through a $1000\ \mu\text{m}$ diameter fiber. 3.5% gelatin (60 bloom, 175 bloom, 300 bloom) was used as the target. The fiber was located 1 mm above the gel surface. All data are mean \pm standard deviation of 5 samples.

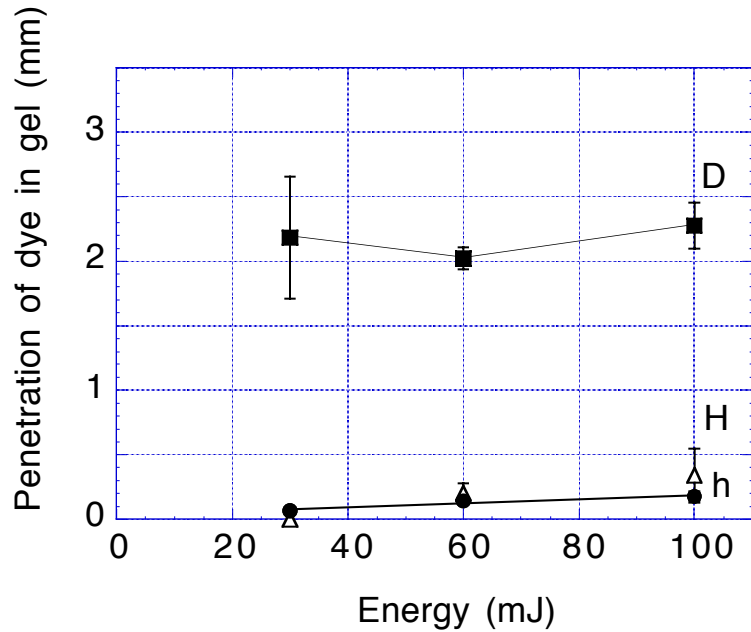


Figure 3. Effect of energy: Penetration of dye in clear gel as a function of the laser pulse energy. The squares (D), triangles (H), and circles (h) present the dye distributions in their own specific directions, cf., Figure 1(b). Absorption coefficient was 300 cm^{-1} . Ten pulses of the laser energies (30 mJ, 60 mJ, 100 mJ) at 3 Hz were delivered through a $1000 \mu\text{m}$ diameter fiber. 3.5% gelatin (175 bloom) was used as the target. The fiber was located 1 mm above the gel surface. All data are mean \pm standard deviation of 5 samples.

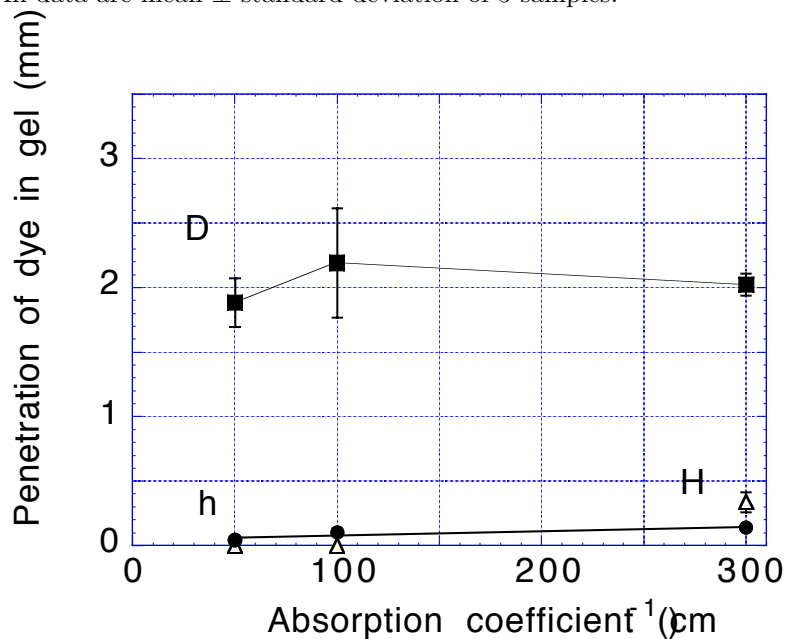


Figure 4. Effect of absorption coefficient: Penetration of dye in clear gel against absorption coefficient. The squares (D), triangles (H), and circles (h) present the dye distributions in their own specific directions, cf., Figure 1(b). Absorption coefficients were 50 cm^{-1} , 100 cm^{-1} , and 300 cm^{-1} . Ten pulses of 60 mJ laser energy at 3 Hz were delivered through a $1000 \mu\text{m}$ diameter fiber. 3.5% gelatin (175 bloom) was used as the target. The fiber was located 1 mm above the gel surface. All data are mean \pm standard deviation of 5 samples.

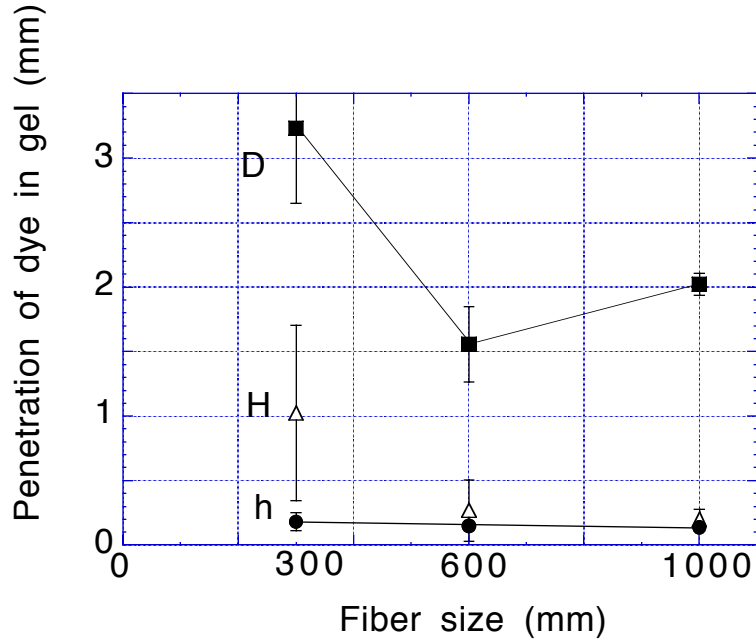


Figure 5. Effect of fiber size: Penetration of dye in clear gel plotted against fiber size. The squares (D), triangles (H), and circles (h) present the dye distributions in their own specific directions, cf., Figure 1(b). Absorption coefficient was 300 cm^{-1} . Ten pulses of 60 mJ laser energy at 3 Hz were delivered through the fibers with 300 μm , 600 μm , and 1000 μm diameters. 3.5% gelatin (175 bloom) was used as the target. The fibers were located 1 mm above the gel surface. All data are mean \pm standard deviation of 5 samples.

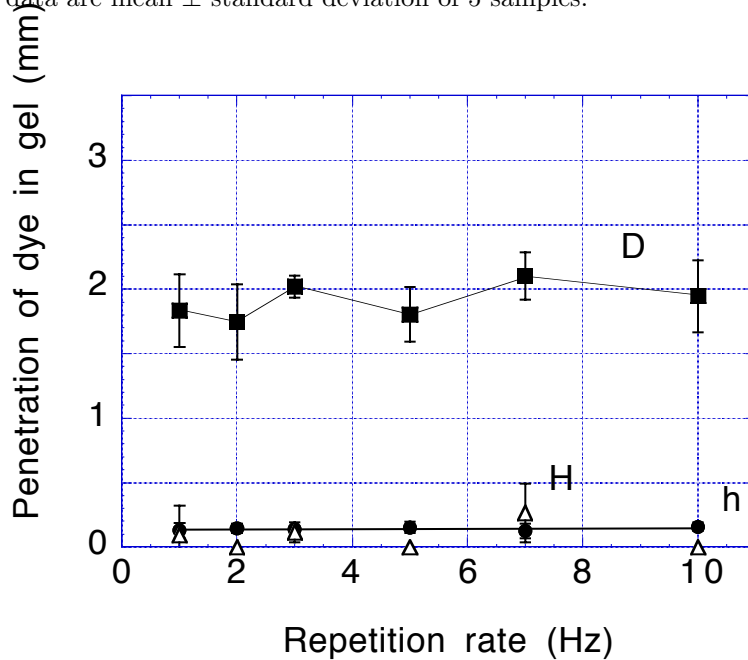


Figure 6. Effect of repetition rate: Penetration of dye in clear gel as a function of repetition rate. The squares (D), triangles (H), and circles (h) present the dye distributions in their own specific directions, cf., Figure 1(b). Absorption coefficient was 300 cm^{-1} . Ten pulses of 60 mJ laser energy operating at 1–10 Hz were delivered through a 1000 μm diameter fiber. 3.5% gelatin (175 bloom) was used as the target. The fiber was located 1 mm above the gel surface. All data are mean \pm standard deviation of 5 samples.

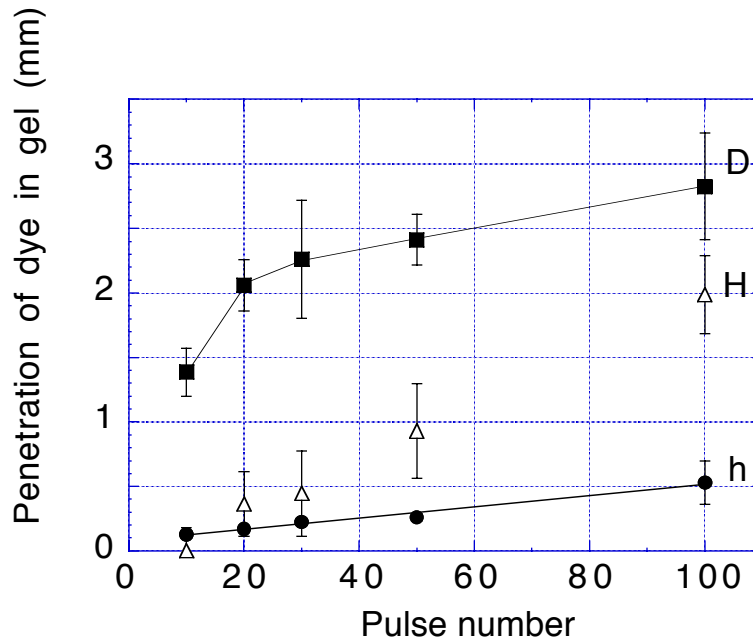


Figure 7. Effect of pulse number: Penetration of dye in clear gel against pulse number. The squares (D), triangles (H), and circles (h) present the dye distributions in their own specific directions, cf., Figure 1(b). Absorption coefficient was 300 cm^{-1} . 10–100 pulses of 60 mJ laser energy at 3 Hz were delivered through a $1000\text{ }\mu\text{m}$ diameter fiber. 3.5% gelatin (175 bloom) was used as the target. The fiber was located 1 mm above the gel surface. All data are mean \pm standard deviation of 5 samples.

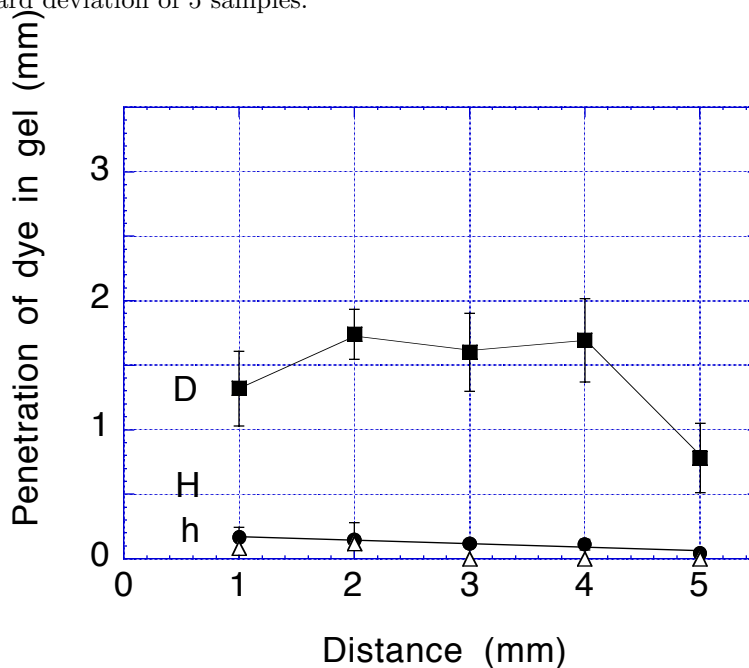


Figure 8. Effect of fiber position: Penetration of dye in clear gel as a function of the distance between the fiber tip and the gel surface. The squares (D), triangles (H), and circles (h) present the dye distributions in their own specific directions, cf., Figure 1(b). Absorption coefficient was 300 cm^{-1} . Ten pulses of 60 mJ laser energy at 3 Hz were delivered through a $1000\text{ }\mu\text{m}$ diameter fiber. 3.5% gelatin (175 bloom) was used as the target. The fiber was located 1–5 mm above the gel surface. All data are mean \pm standard deviation of 5 samples.

4. DISCUSSION

The aim of this study was to identify the mechanisms of PADD. This study was initially motivated by using laser-induced acoustic pressure to drive clot-dissolving enzymes into clots or vessel walls to enhance the efficiency of laser thrombolysis. We investigated the effects of the laser parameters on the spatial distribution of delivered drug using a gelatin-based thrombus model. A simple method to identify the mechanisms of PADD is presented. This method is based on measuring the spatial distribution of delivered dye in clear gel samples. Normally, deeper penetration was accompanied by louder popping sounds.

Cavitation bubble formation in this study is similar to that of a Q-switched holmium laser in water. The absorption coefficient of the holmium laser light at $2.1\ \mu\text{m}$ is $30\ \text{cm}^{-1}$. The Q-switched pulse length is about $1\ \mu\text{s}$ and therefore comparable to those used in this study. In this study and in those of van Leeuwen the cavitation bubbles are formed at the fiber tip after the laser pulse ($\sim 1\ \mu\text{s}$) due to the laser energy absorption by the liquid.¹ This study suggests that a Q-switched holmium laser may be used for PADD, although Figure 4 indicates the penetration will be half as deep as that of a $577\ \text{nm}$ pulsed dye laser in blood (absorption coefficient is $300\ \text{cm}^{-1}$). The pulse duration for the free running holmium laser is much longer ($\sim 250\ \mu\text{s}$) and has completely different dynamics because the bubble is formed during the laser pulse.

The mechanical strength of the gel samples becomes greater with increasing time. For example, a sample stored in a refrigerator for three days may be harder than one stored for one day. That is the reason that the data in Figure 8 are not comparable to those in the rest of figures. The samples used for the data in Figure 8 were stored for three days before the ablation, and the others were stored for one day.

Figure 1(b) shows the section of delivered dye in clear gel. The stained areas for the spatially unconfined geometry consisted of two parts: an inverted hemisphere with a diameter D and height h inserted on the surface of the gel, and some colored cracks below the hemisphere. The hemisphere looked like a kind of dye-gelatin mixture under a microscope. It couldn't be washed away by clear oil or wicked off by a piece of tissue paper. Therefore, we defined it to be uniform penetration without damage. The shape of colored cracks was not reproducible, and the width was less than the diameter D . We infer that the hemispherical stained areas are due to the forceful expansion and collapse of cavitation bubbles, and the colored cracks follow the collapse after the gel structure is cracked. Additionally, the height h increases or decreases linearly, but the H varies non-linearly. We observed that the hemispherical dye-gel mixture was taken off from a sample after an accidentally violent mechanical vibration, and a hemispherical crater was observed at that place. The results that the diameter D is relatively independent of the laser energy and absorption coefficient, while the height h depends on these parameters may imply that the collapse of the cavitation bubbles also plays a very important role in the formation of the hemisphere before the cracking of the gels.

The pulse number affects the penetration significantly. In a comparison of Figure 7 with Figure 3, we find that a similar delivery can be achieved by using $60\ \text{mJ}$ laser energy delivered by a $1000\ \mu\text{m}$ fiber and 10 additional pulses instead of using $100\ \text{mJ}$ laser energy. This suggests that a similar delivery may be achieved by using lower energy with increasing pulse number, rather than using higher energy.

Usually, the spot size of the laser beam on the ablated target is an important parameter for the pulsed laser ablation of tissue. However, we investigated the effect of the fiber size on the delivery instead of the spot size. It was impossible to deliver laser beam directly to the target, since the penetration depth for the solution ($50\text{--}300\ \text{cm}^{-1}$) was $33\text{--}200\ \mu\text{m}$, and the cavitation bubbles were formed right at the fiber tip. Therefore, the spot size on the target has no bearing on the process of PADD, but rather the fiber size determined the radiant exposure. The radiant exposures produced by a $300\ \mu\text{m}$ fiber were about eleven times those produced by a $1000\ \mu\text{m}$ fiber. The bubble grew to a maximum size, and then collapsed. The collapse of cavitation bubbles produced acoustic transients and high pressure shock waves. The shock waves directed toward the solution surface may cause spallation.

Comparing Figure 3 with Figure 5, we find that a similar delivery can also be achieved by using a 300 μm fiber with 60 mJ laser energy rather than a 1000 μm fiber with 100 mJ laser energy. This promises that a laser delivery catheter can be made smaller, and the process of PADD may be safer since a lower energy can be used to achieve a similar delivery with a smaller fiber.

5. CONCLUSION

In this study, we have demonstrated that laser-induced acoustic pressure can be used to drive drug into tissue, and we identify the mechanisms of PADD. Several conclusions can be drawn from this study:

- The penetration of dye in gel is proportional to the laser energy, absorption coefficient, and pulse number.
- Increasing the strength of the material and the distance between the fiber tip and the target surface reduces the extent of the delivery.
- While the dye can be driven a few millimeters into the gel in both the axial and radial direction, the penetration is less than 500 μm when the gel surface remains macroscopically undamaged.
- The penetration mainly depends on the radiant exposure.
- Similar delivery can be achieved by using less energy through a smaller fiber or with additional pulses.

REFERENCES

1. T. van Leeuwen, *Bubble Formation During Pulsed Mid-Infrared and Excimer Laser Ablation: Origin and Implications for Laser Angioplasty*. PhD thesis, Rijksuniversiteit te Utrecht, 1993.
2. S. L. Jacques and G. Gofstein, "Laser-flash photographic studies of Er:YAG laser ablation of water," in *SPIE Proceedings of Laser-Tissue Interaction II* (S. L. Jacques, ed.), vol. 1427, pp. 63–67, 1991.
3. R. de la Torre, "Intravascular laser induced cavitation: A study of the mechanics with possible detrimental and beneficial effects," Master's thesis, Harvard–M. I. T. Division of Health Sciences and Technology, Cambridge, MA, 1993.
4. K. Gregory, "Laser Thrombolysis," in *Interventional Cardiology* (E. J. Topol, ed.), vol. 2, ch. 53, pp. 892–902, W. B. Saunders Company, 1994.
5. H. Shangguan, A. Shearin, and S. A. Prahl, "Visualization of photoacoustic drug delivery dynamics," *Lasers Surg. Med.*, vol. S7, pp. 4–5, 1995 (abstract).